Geolocation Assessment of MERIS GlobCover Orthorectified Products

Bicheron Patrice, Virginie Amberg, Ludovic Bourg, David Petit, Mireille Huc, Bastien Miras, Carsten Brockmann, Olivier Hagolle, Steven Delwart, Franck Ranera, et al.

Geolocation assessment of MERIS GlobCover orthorectified products

P. Bicheron[1], V. Amberg[2], L. Bourg[3], D. Petit[2], M. Huc[1], B. Miras[1], C. Brockmann[4], O.Hagolle[5], S. Delwart[6], F. Ranéra[7], M. Leroy[1], O. Arino[7]

1 POSTEL/MEDIAS-France, CNES-bpi 2102, 18 avenue Edouard Belin, 31401 Toulouse Cedex 9, France

2 MAGELLIUM, 24 rue Hermès, BP 12113, 31521 Ramonville Saint Agne, France

3 ACRI-ST, 260 route du Pin Montard, BP 234, 06904 Sophia-Antipolis Cedex, France

4 Brockmann-Consult, Max-Planck-Strasse 1, D-21502 Geesthacht, Germany

5 CNES/CESBIO, bpi 2801, 18 avenue Edouard Belin, 31401 Toulouse Cedex 9, France

6 ESA/ESTEC, Newton 1, Keplerlaan 1, Noordwijk, The Netherlands

7 ESA/ESRIN, via Galileo Galillei, 00044 Frascati, Italy

Abstract

The GlobCover project has developed a service dedicated to the generation of multi-year global land cover maps at 300 meter spatial resolution using as its main source of data the Full Resolution full Swath (300m) data (FRS) acquired by the MERIS sensor on-board the ENVISAT satellite. As multiple single daily orbits have to be combined in one single dataset, an accurate relative and absolute geolocation of GlobCover orthorectified products is required and needs to be assessed. We describe in this paper the main steps of the orthorectification pre-processing chain as well as the validation methodology and geometric performance assessments. Final results are very satisfactory with an absolute geolocation error of 77 meters rms and a relative geolocation error of 51 meters rms.

1 Introduction

Wide field-of-view sensors such as the Advanced Very High Resolution Radiometer (AVHRR), VEGETATION, MODerate Imaging System (MODIS), Multiangle Imaging Spectro-Radiometer (MISR) and Medium Resolution Imaging Spectrometer (MERIS) provide a near daily global coverage of the Earth with an appropriate resolution to derive land cover or land cover change. These main sources of data have been used widely in the past to produce land cover maps with AVHRR at 8 km [1] and 1 km [2] spatial resolution (or ground sampling distance). Unfortunately, the product quality is often limited by the rather poor geometric accuracy of the data. Significant progress in terms of geometric performance has been made more recently at 1 km with MODIS [3] or VEGETATION/GLC-2000 product [4]-[5]. The GlobCover product from the European Space Agency (ESA) goes beyond this with a land cover map using as its main source of data the full resolution (300m) mode data (FRS) acquired over the years 2005 and 2006 by the MERIS sensor on-board the ENVISAT satellite and a service capable of reproducing this product on a multi-year scale.

Distinction in land cover types at global scale uses primarily the seasonal characteristics of vegetation generally based on the temporal dynamics of spectral information acquired by the wide field-of-view sensors. Nevertheless, numerous physical effects - cloud and atmospheric contamination, surface anisotropy- require composing multiple daily orbits into a single data set [6]-[7]. Achieving a high level accuracy relative geolocation is therefore a critical step for each orbit. In addition, even if absolute geolocation accuracy is not needed in principle for such compositing, the use of the ouput products with a geographical scope is strongly limited and subject to additional errors, such as mislocation of control points [8], if the absolute geolocation accuracy is poor. Therefore, major efforts are made in geometric correction and the assessment of geolocation accuracy whatever the sensors – AVHRR [9]-[10], ATSR [11]-[12], VEGETATION [13], POLDER [14], MODIS [15]-[16], MISR [17]-[18], WindSat [19], SSM/I [20]. The impact of mis-registration effects has also been studied on composited data [21]-[22] as well as on land cover [23]-[24] and land cover change [25]-[26].

The MERIS mission has been designed with the primary objective to better understand the role of oceans and ocean productivity in the climate system. The initial accuracy specifications for MERIS absolute geolocation of 2000 m is sufficient for observation of ocean colour. Due to its 15 spectral bands with a high radiometric resolution in the optical domain and its dual spatial resolution, MERIS also offers great opportunities for observation over land. Over the terrestrial ecosystems, the geolocation performance needs to be largely improved with respect to the initial specifications over ocean. Regular efforts concerning the MERIS pointing as well as the attitude on–board software have been made. Simultaneously, short studies [27]-[28] were performed so as to verify the geometric performance over specific time periods and these showed that absolute geolocation root mean square errors stayed within the ranges of 170 meters up to 500 meters. All these aforementioned geometric correction assessments were based either on the original navigation model of MERIS, or on limited scenes sampling, and not on a systematic projection grid. The recent development of Accurate MERIS Ortho-Rectified Geolocation Operational Software–AMORGOS [29] provides geolocation information for every image pixel of the Full Resolution product (FR) using a Digital Elevation Model (DEM) named Global Earth Topography And Sea Surface Elevation at 30 arc second resolution – GETASSE30 [30]. As the GlobCover processing integrates AMORGOS coupled with a cartographic projection system taking into account the local elevation, an extensive study must be achieved in order to assess the performance of such an approach.

In this paper, we estimate the absolute and relative geometric accuracy of GlobCover products. Section 2 provides an overview of the baseline processing of MERIS Level 1B. The orthorectification modules are then described including the AMORGOS geolocation and cartographic projection modules. The validation process is presented in Section 3. Absolute and relative geometric accuracies of GlobCover products are requested to be better than 150 m (i.e. half a pixel) so as to deliver a final land cover map of high quality. Our objective is therefore to evaluate whether these requirements are fulfilled on a global basis. These assessments are performed through the processing of disparity measurements in column and line shifts between the orthorectified images and reference independent images acquired over sites located at different latitudes, at different times and with different

topography and cloud coverage. The validation process is done by an independent team of the GlobCover project different from the entity responsible for the production of orthorectified images. Section 4 describes the results in relative and absolute accuracy following several simple statistic criteria.

2   MERIS GLOBCOVER orthorectification

2.1   Description of the MERIS level 1B processing

On-board ENVISAT launched in 2002, MERIS is a wide field-of-view push broom imaging spectrometer measuring the solar radiation reflected by the Earth in 15 spectral bands from 412.5 nm to 900 nm. Each of these 15 bands is programmable in position and in width. The instrument has a field of view of 68.5 degrees and covers a swath width of 1150 km at a nominal elevation of 800 km enabling a global coverage of the Earth in 3 days. The wide field-of-view is shared between five identical optical modules arranged in a fan shape configuration, each camera covering a 14 degree field of view with a slight overlap (see Figure 1). The image is constructed using the push-broom principle: a narrow strip of the Earth is imaged onto the entrance slit of the spectrometer, defining the across track dimension. The motion of the satellite together with the acquisition time sampling provide the along track dimension. The spectral dimension is achieved by imaging the entrance slit of each spectrometer via a dispersing grating onto a 2-D CCD.

The instrument resolution is 290 m (along track) x 260 m (across track) at nadir point; corresponding data are referred to Full spatial Resolution (FR). Data at a coarser resolution are systematically generated on-orbit by spatial (across-track) and temporal (along-track) averaging of groups of 4 x 4 pixels yielding a Reduced spatial Resolution (RR) of 1160 m by 1040 m. The RR data are transmitted to ground on a global basis whereas the FR data are limited to regional coverage, focusing on land surfaces and coastal areas.

The level 1B MERIS Full Resolution full Swath (FRS) product contains calibrated top of atmosphere gridded radiances over the full sensor's swath. The radiometric processing [31] includes several steps,

namely detection of saturated pixels, stray light correction and estimation of spectral radiances. The geolocation processing is split in five steps (product limits, tie points on Earth location, elevation retrieval, re-sampling, sun glint) which are summarized below.

Due to the sharing of the field-of-view by five identical sensors, there is no spatial continuity in the data acquired by the instrument: the slight overlap between adjacent cameras, as well as the slight inter-camera misalignment, requires spatial re-construction to be provided for the users with spatially continuous and regularly sampled MERIS products, at Level 1 or higher. This re-construction is based on an ideal instrument acquisition grid: the along-track sampling is the actual instrument one, the across-track sampling is defined as perpendicular to the satellite track and evenly spaced on-ground.

The product grid is computed from satellite navigation and attitude data allowing computation of the intersection of the instrument field-of-view with the Earth surface represented by the WGS 84 reference ellipsoid at zero elevation. The retrieved instantaneous field-of-view swath is sampled with a constant distance on-ground to build the product pixels (Figure 2). Correspondence with instrument pixels can then be done on the basis of across-track pointing angle. This process is actually done on only a sub-set of the product pixels, called the tie points so as to improve storage efficiency. The tie points grid has 71 tie points across track. It corresponds therefore to a 16 x 16 sub-grid of the RR product grid and to a 64 x 64 sub-grid of the FR product grid. For these tie points, the geolocation data (longitude λ, latitude ϕ) is complemented with illumination and observation angles (θ_s, φ_s, θ_v, φ_v) and other geophysical information (elevation above the reference ellipsoid – meaning sea surface height for ocean pixels, surface roughness, first order parallax correction terms due to elevation, meteorological information). The regular time sampling provides a quasi-even distance on Earth. Variations of the along-track sampling step of up to about 3% are due to the orbital motion of the satellite and the ellipsoidal shape of the Earth, across-track distance between pixels being regular by construction.

6

It must be noted here that since the level 1B product grid is filled by a nearest neighbour method from the instrument grid with a slight spatial over-sampling, the same instrument sample can be found several times in the same level 1B product (it is then identified as a 'duplicate' pixel within the level 1B product flags).

2.2 The geolocation and cartographic projection modules

The geolocation principle described in previous section was primarily intended to fulfil requirements for the Ocean community, the initial accuracy specification for MERIS absolute geolocation being 2000 m. Such requirements are not sufficient for the Land community. ESA has put some efforts to improve the on-board attitude software as well as geolocation monitoring. A slow degradation in the MERIS absolute geolocation was observed before December 2003 - the mean error was about 500 meters - mainly in the across-track direction [28]. On December 2003, the on-board attitude software change resulted in an immediate improvement of the geolocation to around 270 meters. A modification of the MERIS pointing auxiliary data took place on January 2005 which further improved geolocation performance of standard products to about 170 m [27]. At the same time, ESA initiated the development of the AMORGOS post-processor. Its purpose was to provide accurate per-pixel geolocation information – longitude λ, latitude ϕ, elevation h – accounting for the Earth surface elevation and actual satellite navigation and attitude control, generally not available at the time of near-real time MERIS data processing. Furthermore, the geolocation information was provided following the pointing characteristics of the original instrument pixel regardless of the spatial re-sampling described in the previous section, even if the data were still provided in the re-constructed regular image grid. Using MERIS FRS products as input, the MERIS Full Swath Geo-located (FSG) products are generated through AMORGOS proceeding as follows:

1. identify the original instrument pixel, on the basis of the FRS product information and of the auxiliary data used during the re-sampling step of the FRS product generation,

2. compute Satellite location and actual attitude at acquisition time,

3. using the instrument pixel's characterised pointing direction, follow its line-of-sight until it intersects the Earth's surface, represented by the DEM GETASSE30 on top of the reference

ellipsoid (Figure 3). This elevation model is a composite dataset using the SRTM30 dataset [32], ACE dataset [33], Mean Sea Surface (MSS) data [34] and the EGM96 ellipsoid [35].

The main differences with the MERIS standard products geolocation are:

1. satellite ephemeris and attitude are re-computed from best possible quality sources in order to ensure best achievable accuracy,

2. information (longitude λ, geodetic latitude ϕ and elevation h) are provided for each image pixel,

3. pixel location is derived taking into account the actual Earth surface elevation along the viewing direction,

4. information is retrieved according to the original instrument pixel, regardless of the image re-gridding.

The MERIS FSG images are then projected on a cartographic system. The plate-carrée coordinate reference system (CRS) has been chosen since the final land cover product has its main use in global thematic mapping that is very often projected in this CRS. The reference ellipsoid is WGS 84 assuming respectively an equatorial (R_e) and polar radius (R_p) equal to 6378137 m and 6356752.3 m. The grid cells have an angular pixel resolution Res_{deg} and a spatial size defined by its height and width:

$$
\begin{aligned}
height &= r \times 2\pi / 360 \times Res_{deg} \\
width &= R_e \times \cos(\phi) \times 2\pi / 360 \times Res_{deg}
\end{aligned}
\tag{1}
$$

with $r = \dfrac{R_e \times R_p}{\sqrt{R_e^2 \times \sin^2(\theta_c) + R_p^2 \times \cos^2(\theta_c)}}$ and $\theta_c = \arctan(1-f)^2 \times \tan(\phi)$

with $f = \dfrac{(R_e - R_p)}{R_e}$ and $Res_{deg} = 1/360$

The general concept for the image georefencing has already been described in the literature [36]-[9]. One must consider:

- a direct location function *f(l, p, h)* producing the geographical coordinates *(λ, φ)* in the reference system associated to a cell of the georeferenced image for any point located in the raw image by its line *l*, column *p* and elevation *h*. In the MERIS case, it is derived through the AMORGOS post-processor.

- a reverse location function $f^{-1}(λ, φ)$ applied to every cell of geographic coordinates determining at which raw image line *l* and column *p* the cell is imaged.

As the grid of MERIS FSG product is not evenly spaced in angle and because of the parallax defects, the reverse function is not strictly defined and may only be predicted. We use two 4th degree polynomial functions *L(λ, φ)* and *P(λ, φ)* linking line *l* and column *p* of any pixel from the MERIS FSG image as a function of latitude *φ* and longitude *λ*. The coefficients of these predictive polynomial functions are determined over a sub-sampling of the MERIS FSG grid through an equation system built considering one point out of ten and solved using a least-squares minimisation procedure. As recommended in [37]-[38], these functions are computed on two grids of constant elevation H_{min} and H_{max} representing respectively the minimum and maximum elevation value on the concerned DEM.

The retrieval of the pixel line *l* and column *p* in the MERIS FSG image of the current cell *(λ, φ)* is done through an iterative approach. First, an estimation of line and column is processed thanks to the reverse location function defined by the predictor polynomial functions *L(λ, φ)* and *P(λ, φ)*. For the estimated line and column, the corresponding latitude and longitude are interpolated through a bilinear sampling over a 2 x 2 pixels neighbourhood in the MERIS FSG image. These geographic quantities are then used for a new estimate of the line and column of the current cell. Successive iterations are repeated until a predefined tolerance is reached. The final estimate of line *l* and column *p* at the current elevation *h* is derived from a linear interpolation between the results obtained at H_{min} and H_{max}. In case the polygon crosses the meridian ± 180°, the continuity in longitude is ensured adding a modulo 360°. The final radiometry *DN (l, p)* is computed with a bi-cubic interpolation algorithm over a 4 x 4 pixels neighbourhood.

3 Validation process

3.1 Methodology

Two kinds of validation are performed: 1) verification of co-registration accuracy of orthorectified MERIS images (or relative geolocation accuracy), 2) verification of absolute geolocation accuracy. In both cases, the validation is performed by comparing the ortho-rectified MERIS images with some geo-located reference data. For each MERIS-reference data pair, the methodology is based on an automatic selection of sampling points (thousands of points by pair) on a regular grid with tuneable sampling rate. This detection is performed by computing similarity measurements between images. Quantitative assessments of relative and absolute geolocations are then performed in terms of disparity measurements (column and line shifts) between sampling points of images.

The correlation measurement is performed using the MEDICIS CNES correlation tool. For each sampling point, the principle is to compute a similarity measurement between a master image (or reference image) and a slave image, that is translated by incremental steps with respect to the master image (Figure 4). Deformations applied by MEDICIS are only translations here. Shifts in line and column are estimated in a local window (50 x 50 pixels) centred on each correlation point by evaluating in an iterative process the translation that maximizes the similarity criterion between the master image and the slave image [39]-[40]. For our study, we have chosen the standard correlation as the similarity criterion.

The disparity measurement between two images is generally performed on a great number of sampling points. To assure the accuracy of the disparity estimate, several types of pixels are not taken into account in the final statistics. First, ocean flagged pixels are removed considering that the similarity measurements over ocean are often not accurate due to the target temporal variability between two acquisitions and its lack of texture. Invalid flagged pixels, including especially clouds present in both images, are not taken into account. Sampling points with a low similarity rate (*i.e.* low confidence rate in disparity measurements) are also excluded from the final statistics: the accuracy of similarity measurements between two images can decrease if some changes have occurred between the two

10

acquisitions. Global shifts between the images are finally computed by averaging locally measured shifts obtained on all retained sampling points. This average reduces the bias of correlation and produces an accurate shift measurement.

In case of relative geolocation accuracy assessment, the reference products are naturally MERIS images acquired over the same area at a different time. In case of absolute geolocation accuracy assessment, the reference images are data produced by the ETM+ multi-spectral sensor on-board LANDSAT 7. The resolution is 30 m and only band B4 (760-900nm) is used. The choice of this band is made so as to ensure a maximum spectral coverage with the 865 nm spectral channel B13 of MERIS and hence a maximum similarity between images [41]. LANDSAT images have been geolocated and orthorectified with *RMSE* accuracy inferior to 50 m [42][43]. Since LANDSAT products are better resolved than those of MERIS, LANDSAT images have been rescaled to 300 meters (MERIS products resolution) by spatial averaging. Thus absolute validation is done at MERIS resolution.

Two main advantages of such a study can be highlighted: first, a high precision of disparity measurements is provided by MEDICIS. In fact, the intrinsic correlation error of MEDICIS (internal CNES studies) is evaluated to 0.025 pixels (versus 0.3 pixel at best for a manual selection of sampling point). Second, the estimate of the disparity between images is made very accurate by averaging on a high number of sampling points. In our study, the sampling rate is 10 pixels corresponding to approximately 150 000 sampling points per pair automatically selected and evaluated. Since ocean pixels, invalid pixels or sampling points with a low similarity rate are excluded, only about 20% are kept in the final statistics.

The disparity measurements provided by the correlation tool are produced by several error contributions distinguishable according to the assessment case. For relative and absolute location error assessments, the correlation error of MEDICIS must be considered. In the case of relative error assessment, we must add the co-registration error of MERIS data. In the case of absolute error assessment, we must take into account the registration error of MERIS data with respect to the

reference data as well as their own geolocation error (<50 m). The location precision is directly derived from mean shift measurements in row and column.

3.2 Reference images selection

Geolocation errors can be induced theoretically by several phenomena such as measurement errors of satellite ephemeris and attitude, lack of DEM precision when processing geolocation and projection, and instrumental drifts. As MERIS is composed of 5 independent CCD sensors observing 5 adjacent areas, some independent location errors can also occur between the different parts of the scene imaged by each sensor. This last source has not been investigated in our study. Finally, the test sites have been carefully selected according to:

- Different latitudes and observation dates for the monitoring of the temporal instrumental drifts in latitude.

The measurements quality of MERIS instrument have been rigorously studied and currently monitored in flight [29]. However, some instrumental drifts could occur in latitude and in time, principally because of thermo-elastic effects of the sunlight illumination on the satellite. Such instrumental drift effects on the geolocation accuracy can be highlighted by comparing relative and absolute validation results obtained on sites located at different latitudes and products acquired at different dates.

- Different topographies for the study of the potential relief influence.

Geolocation errors induced by topography can be highlighted by looking for some relations between these errors and the elevation. This study can be performed by computing the joint probability between location error and elevation. From this probability, it is then possible to analyze the location error as a function of elevation and then to highlight a possible relation between topography and geolocation errors. A faster approach consists of comparing geolocation accuracy results obtained on several sites presenting different relief (desert areas, flat lands, mountainous areas, etc.).

- Cloud cover quality and data availability

Cloud pixels are not taken into account in the similarity process (see section 3.1). Thus the selected images must present as few clouds as possible in order to keep enough sampling points for the average

of accurate disparity estimations. Since several images of different sites and for different time periods must be selected, sites with a high revisiting rate must be favoured.

- Sites taken at different longitudes

This aims at verifying that sites located at different longitudes present the same geolocation error.

For the relative validation, about five images per site and per time period are selected providing a total amount of about 100 orthorectified MERIS images – 5 images × 5 sites × 4 time periods – representing theoretically 200 MERIS pairs. For each period, the images must be acquired on different orbits. The maximum common area between two images is 10° x 10° due to GlobCover tiling [44]. For each site, the four following time periods have been considered over the years 2004 and 2005:

- from December 1st to December 15th and from January 1st to January 7th for the Winter season taking the northern hemisphere as reference
- from April 8th to April 30th for Spring
- from June 1st to June 30th for Summer
- from October 1st to October 21th for Autumn.

According to the criteria outlined above, five sites have been chosen: Madagascar, Tunisia, Spain-Morocco, Romania-Ukraine, Poland-Sweden. Table 1 represents the number of selected MERIS images per site and derived pairs that have been successfully geo-located and orthorectified. Finally, 146 pairs out of a total of 200 theoretical pairs have been formed for the relative validation which produces a dataset sufficient for the purpose of the geolocation study. We were not able to select the full initial set of 5 MERIS images for each site and season for the following reasons:

- For some sites and seasons (e.g. northern Europe in winter or autumn), it is very difficult to select 5 images with few clouds.
- At the time of this study, the data collection for the year 2005 was not completely delivered. Especially, the winter season (January, February and March) was very poorly covered.

4 Results

4.1 Relative validation results

4.1.1 Global results

Each pair is built by associating one orthorectified MERIS image for one site and one season with another image present for the same site at the same season but not on the same day. For each pair, quality criteria (arithmetic means, standard deviations and *RMSE* errors in latitude and longitude as well as the global *RMSE*) have been estimated by averaging results computed through MEDICIS on all sampling points: it results in 146 disparity measurements. On this experimental material, global statistics have been computed as follows and summarized in Table 2:

- Mean features represent the mean value of the 146 estimated quality criteria.

- Standard deviation features represent the standard deviation of the 146 estimated quality criteria.

- Minimum features represent the minimum value of the 146 estimated quality criteria.

- Maximum features represent the maximum value of the 146 estimated quality criteria.

The mean *RMSE* total has a value of 51.6 m with values in latitude and longitude quite similar showing that no specific problem seems to exist in one of these directions. This means that the GlobCover requirement of 150 m is globally satisfied concerning the co-registration quality of FR MERIS products. Standard deviations of *RMSE* are satisfactory with values about 20 m (i.e. small) in latitude and longitude. Moreover, *RMSE* obtained on the whole dataset are very similar. We may therefore be confident in the assessment of the relative geolocation accuracy.

Figure 5 represents the *RMSE* in longitude as a function of *RMSE* in latitude for the 146 pairs: one symbol represents a pair. The bold semi-circle represents the threshold of values required at the beginning of the GlobCover project: pairs located inside the bold semi-circle satisfy the geometric property requirements (i.e. global *RMSE* < 150m). This data representation shows that only 3 pairs among the 146 tested do not satisfy the GlobCover specifications for the MERIS image co-registration: this is a very satisfactory result. The dashed semi-circles correspond to a *RMSE* value of

100 m. About 12% of the pairs are located between 100 m and 150 m. Furthermore, these pairs correspond to desert areas on which it is difficult to perform accurate similarity measurements because of a lack of texture. If these pairs are removed from the dataset, the mean *RMSE* decreases significantly with a mean value of 35 m.

4.1.2 Influence of time, latitude, topography

In this section, we analyze the behavior of MERIS images co-registration errors with time, latitude and topography. In order to highlight a possible degradation of co-registration accuracy with time, the temporal evolution of the *RMSE* in latitude and longitude is represented for the 5 sites (Figure 6). Logically, the relative geolocation results over the desert site of Tunisia are not as good as those obtained on the other sites. For the whole sites, the co-registration errors of MERIS images do not increase in the long term: no relation between seasons and errors is distinguishable. In a short term, *RMSE* variations exist within the seasons. It may arise from directional effects generating radiometric differences that are not corrected in daily images. The similarity measurement may be exaggerated by shifting artificially successive images so as to counterbalance these effects. Range of *RMSE* magnitudes stay globally within the GlobCover specifications. Potential instrumental drifts in time have no effect on co-registration accuracy of MERIS images.

The possible degradation of co-registration accuracy with latitude is analyzed through the representation of the evolution of the same criteria with latitude (Figure 7). The main conclusion is that the co-registration errors of MERIS images for the 4 seasons do not vary with this parameter: no relation between latitude and errors seems to exist. Thus potential instrumental drifts in latitude have no effect on co-registration accuracy of MERIS products. For all seasons, the difference of relative validation results between the site of Tunisia and the other sites, already observed in the previous sections, is clearly visible.

The possible influence of the topography on co-registration accuracy of MERIS images is represented on Figure 8. The site of Madagascar has been selected because of its stressed relief. For a single pair

of images, local disparity measurements of all sampling points located within an interval of 10 m of elevation are averaged so as to relate the *RMSE* to elevation. Elevation is related negatively to geolocation error (higher elevation has smaller error). At the same time, the noise increases with elevation since similar *RMSE* levels are sometimes observed at high elevation (between 1250 and 2000 m) and low elevation (< 500 m). This result is not surprising. First, steeper slopes are generally present at higher elevation generating stronger geolocation errors [23]. Secondly, *RMSE* is probably estimated less accurately at high elevation than at low elevation. In fact, for the tested site, less sampling points are located at high elevation than at low elevation resulting in fewer results on average for high altitude. Nevertheless, the *RMSE* level remains within the 150 m requirement and influence of elevation on geolocation error is therefore acceptable. Residual thin clouds may be present in both images around the correlation point but at different locations. The RMSE peak observed at 1300 m represents an example of this situation.

4.2 Absolute validation results

In this section, a cross-validation of FR MERIS images geolocation accuracy is done using LANDSAT images. This part of the study is not done on the whole dataset. Only images acquired in summer over Spain and Madagascar are tested. Thus 10 pairs are concerned by this study resulting in 10 disparity measurements (one for each pair). For all the pairs of LANDSAT and MERIS images, the same quality criteria as section 3.1 have been estimated by averaging local results computed on all sampling points.

Table 3 summarizes the results obtained on the 10 pairs. The global *RMSE* has a value of 77.1 m inferior to 150 m. Figure 9 represents the *RMSE* in longitude as a function of latitude for the 10 pairs. All pairs are located inside the semi-circle of geolocation validity required by the GLOBCOVER project. A shift in longitude is observed with a mean difference higher in longitude than in latitude. This remark is confirmed by Figure 10 representing the mean difference in longitude as a function of latitude. On this diagram, the scatter plot is almost centered on zero in latitude but not in longitude. It is also seen in Table 3 that extreme values of RMSE are uncommonly more tightened than for the the relative accuracy assessment (104.2 m for the maximum value versus 214.4 m). First, the number of disparity measurements is here significantly lower with only two sites over a single season. In

addition, LANDSAT images do not cover entirely MERIS images resulting in a lower number of sampling points per pair.

5 Conclusions

The co-registration and absolute accuracies of orthorectified MERIS GlobCover products are in agreement with specifications i.e. largely inferior to 150 m. This level of accuracy is achieved thanks to the latest improvements concerning the MERIS on-board pointing and attitude software as well as the development of additional processing modules. First of them, AMORGOS provides geolocation information for every image pixel whereas it was only available at tie points in the FRS image. The cartographic projection tool allows generating surface reflectances in the requested corresponding grid and for every kind of FRS product.

Concerning the assessment method, we have demonstrated that a very accurate control points positioning has been performed thanks to MEDICIS. For each MERIS image, numerous sampling points (typically many thousands) have been selected ensuring an accurate estimation of the absolute geolocation and co-registration accuracy of MERIS images. The study has been done on numerous pairs (146 for the relative validation). No effect on geolocation generated by instrumental drifts in time and latitude exists. This study shows that influence of elevation on the geolocation accuracy remains acceptable either. The use of GETASSE 30 DEM is therefore sufficient. This result may be compared with similar outcome already obtained [36] where orthorectification made with SRTM or another DEM at a better spatial resolution gave similar results. Finally, the respective relative and absolute geolocation accuracies of 51.6 m and 77.1 m are largely in line with the GlobCover specifications. The post-processor AMORGOS coupled with a cartographic projection system integrating the local elevation may be recommended as a standard for the MERIS image processing so as to enhance the development of useful applications over terrestrial ecosystems.

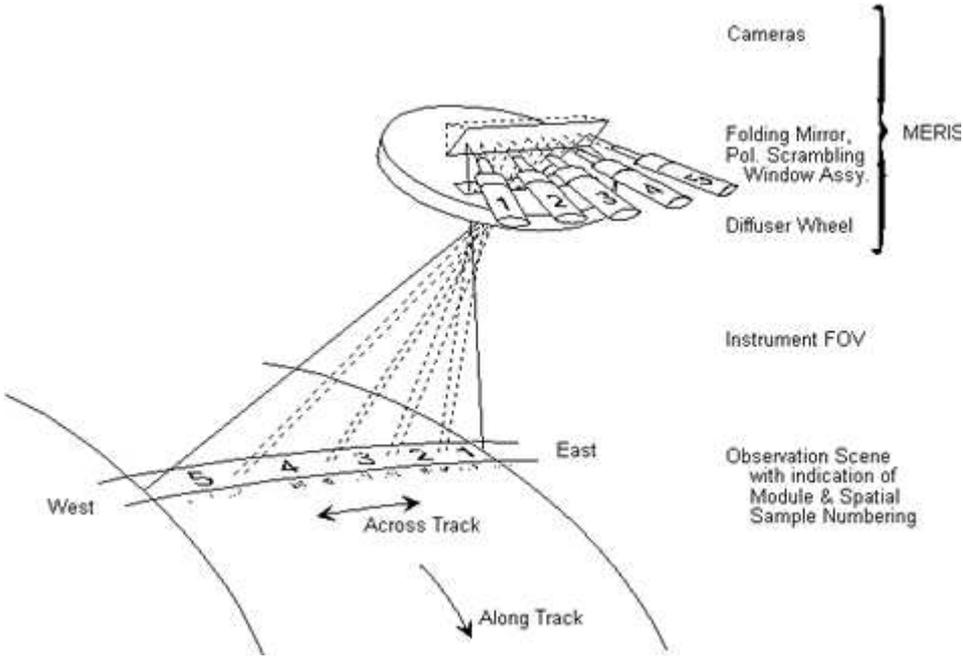# Figures and tables list

6 Figures

Figure 1 - MERIS sensor: FOV, camera tracks, pixel enumeration and swath dimension
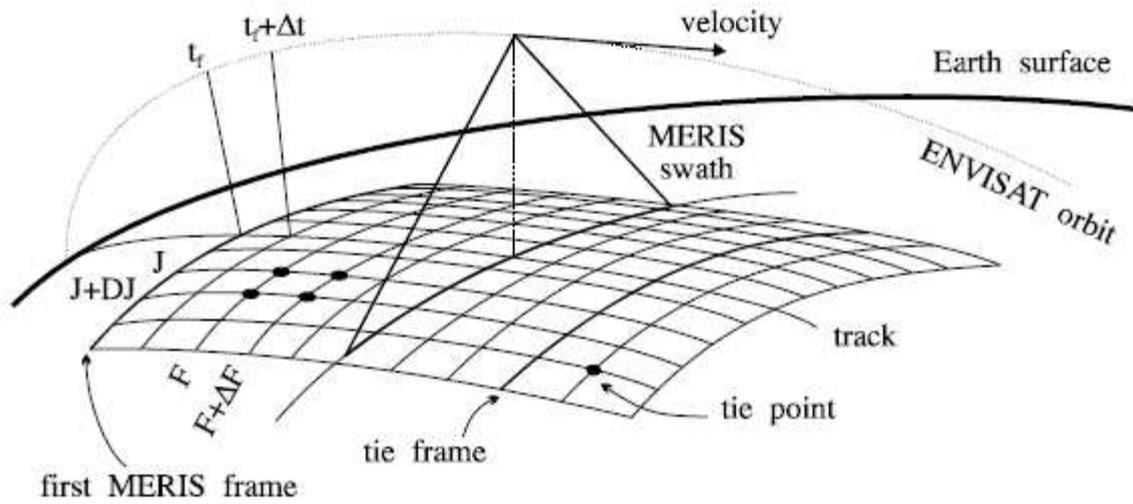
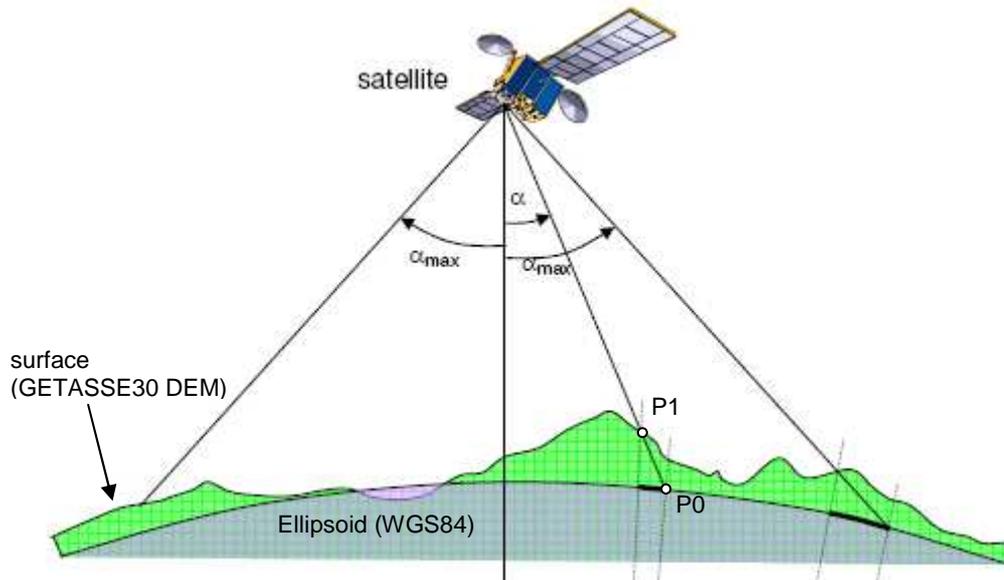**Figure 2 - The MERIS Level 1B tie points grid along the ENVISAT orbit**

Figure 3- AMORGOS geolocation principle and parallax illustration: intersection between the line of sight and the GETASSE 30 DEM. α_{max} , P0 and P1 correspond respectively to the maximum field of view (34.25°), the MERIS standard products geolocation and the AMORGOS geolocation
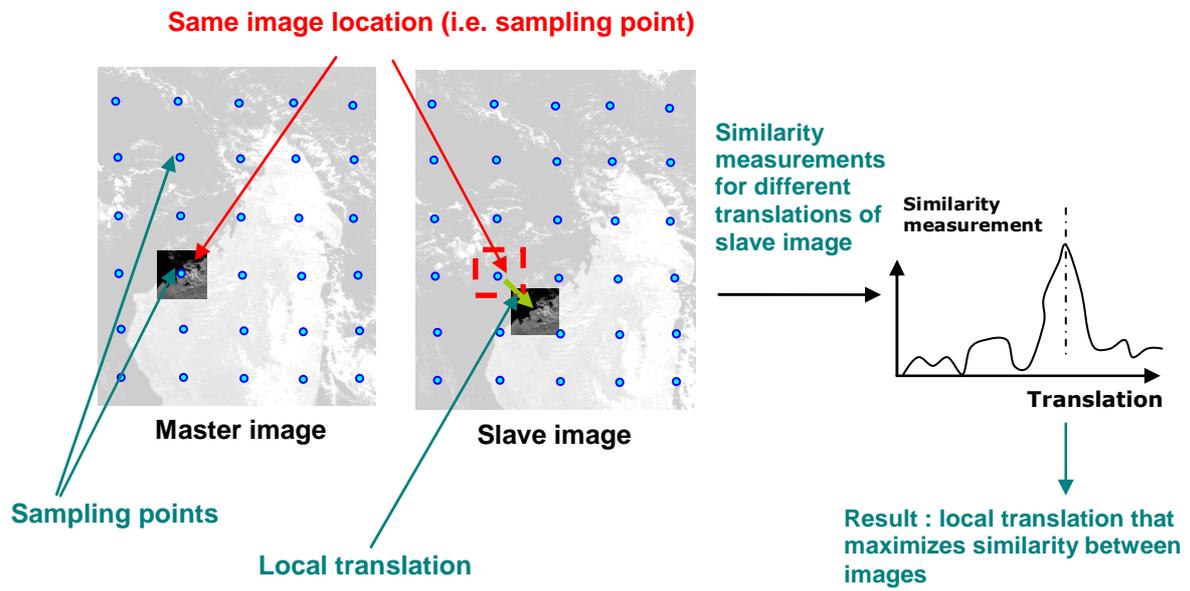
Same image location (i.e. sampling point)

Similarity measurements for different translations of slave image

Similarity measurement

Translation

Master image

Slave image

Sampling points

Local translation

Result : local translation that maximizes similarity between images

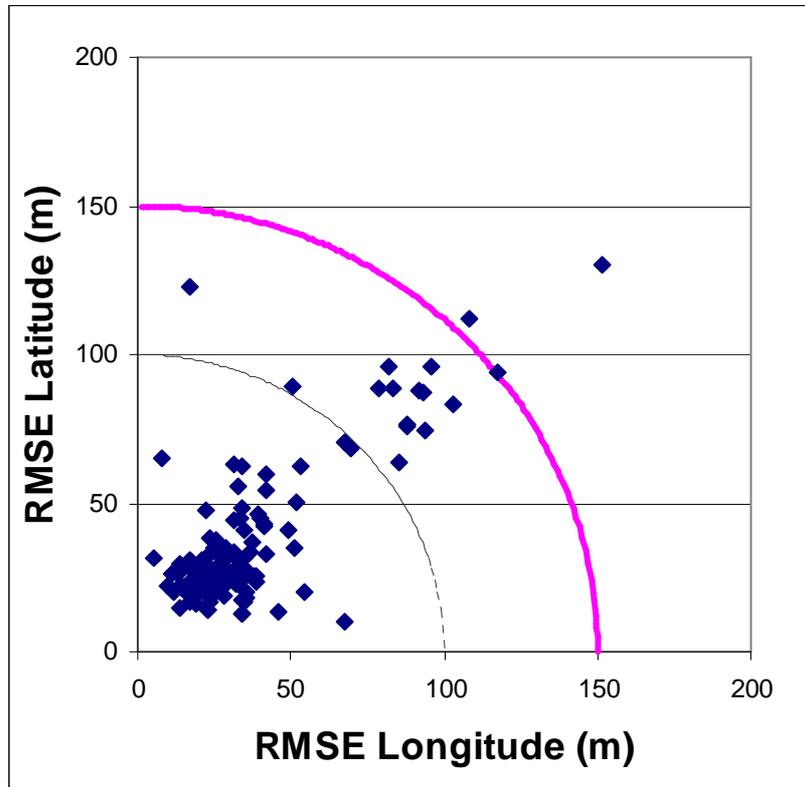**Figure 4 - Determination of line and column shifts with the MEDICIS tool**

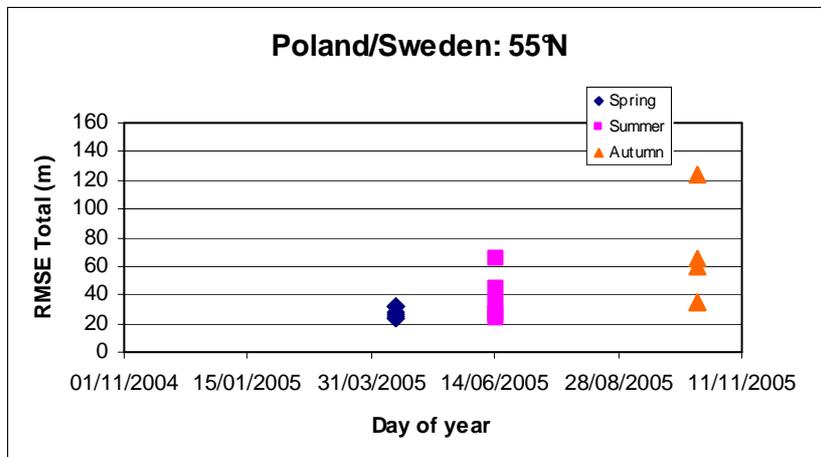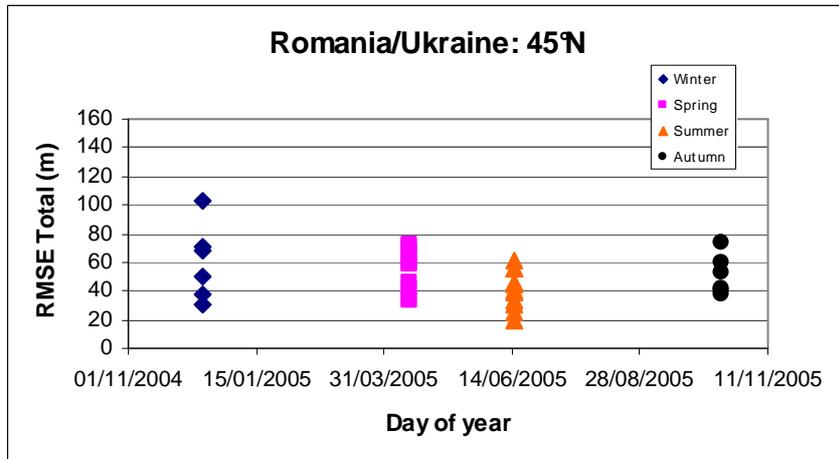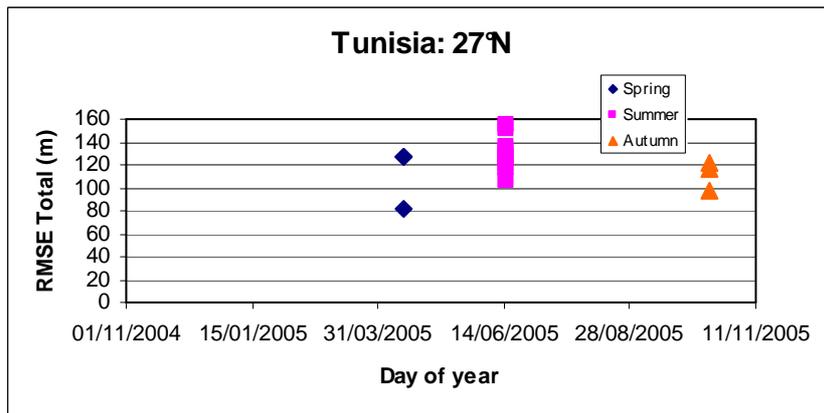**Figure 5 - Global relative accuracy results (unit: meter)**

Figure 6 - Influence of time on the relative geolocation results. A symbol represents a result for one pair of MERIS images.
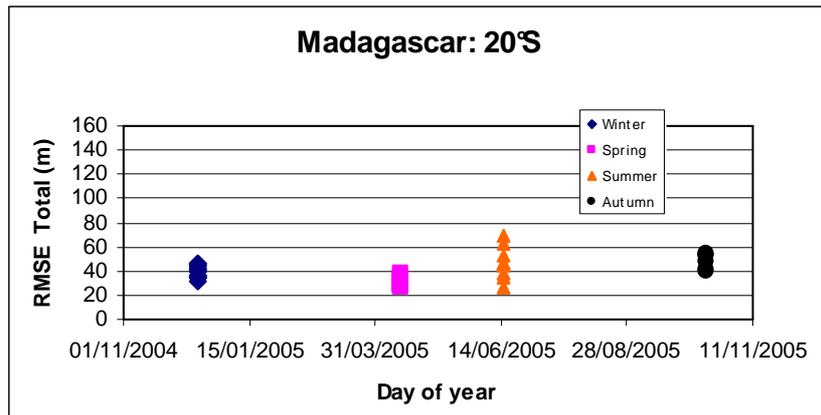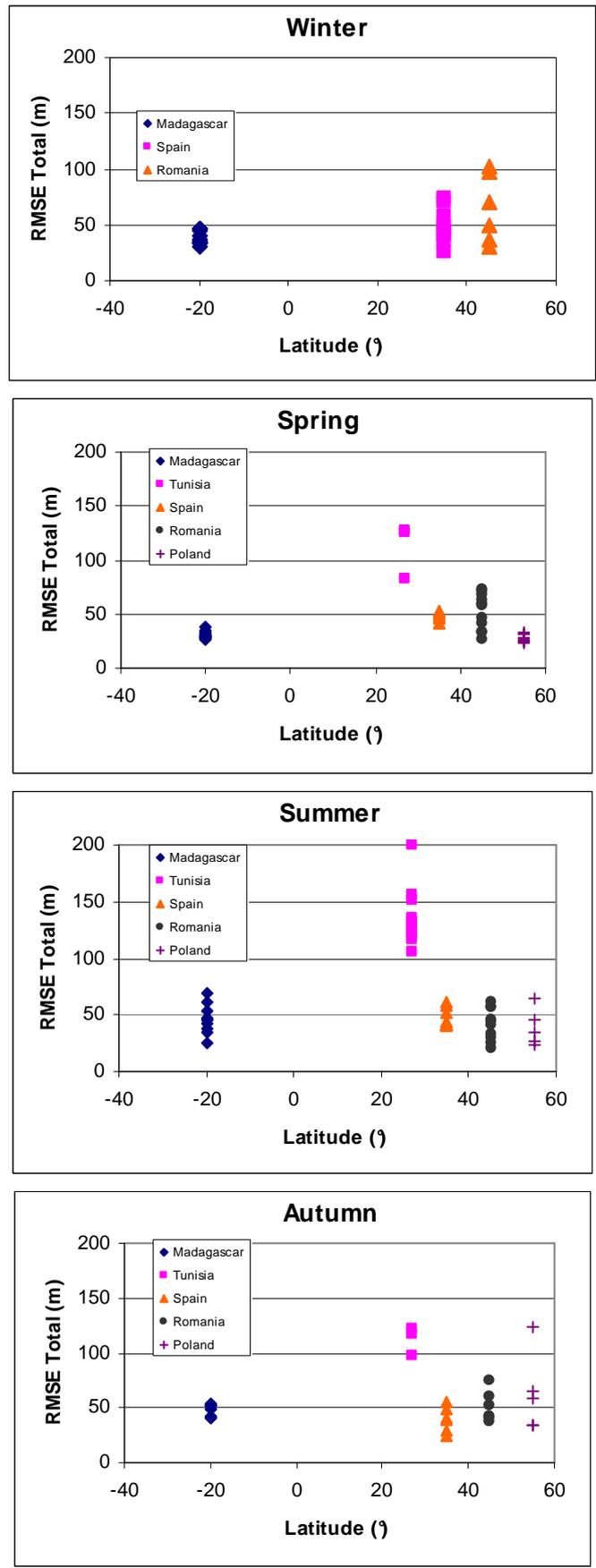
Figure 7 - Influence of latitude on the relative geolocation results. A symbol represents a result for one pair of MERIS images.
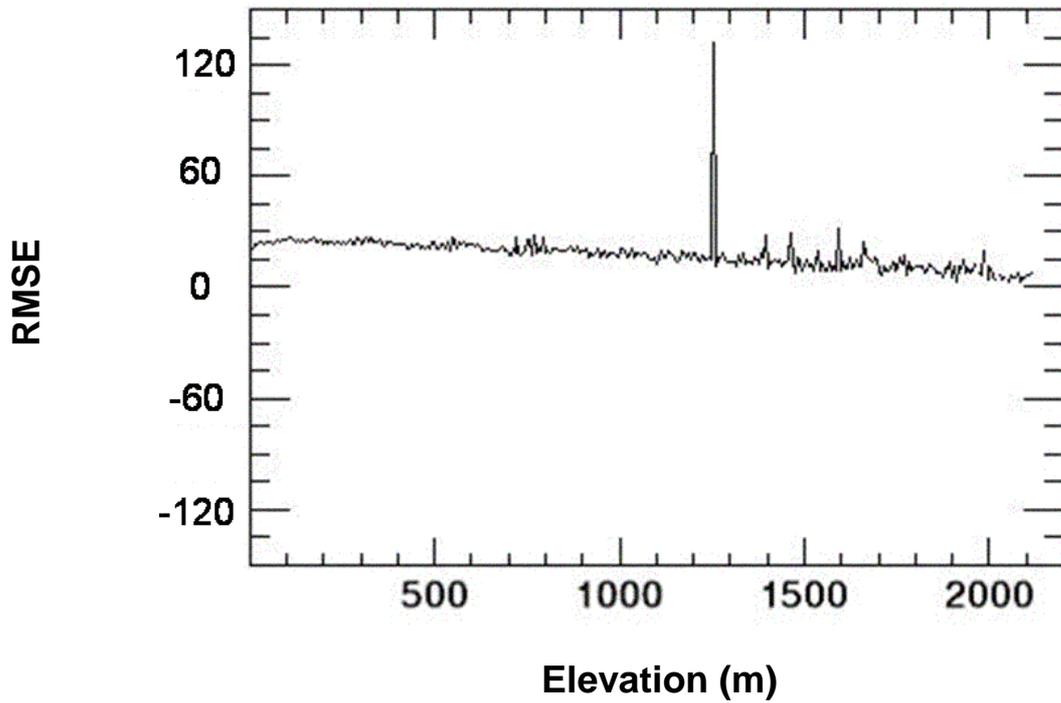
Figure 8 - Influence of elevation on the RMSE (unit: meter) for the relative geolocation results obtained over Madagascar site

Figure 9 - RMSE in latitude as a function of RMSE in longitude for the absolute geolocation assessment (unit: meter)

Figure 10 – Arithmetic mean (shifts) in latitude and in longitude for absolute geolocation accuracy with LANDSAT products (unit: meter). The square symbol corresponds to the mean value

.

7 Tables

Table 1 - Selected dataset

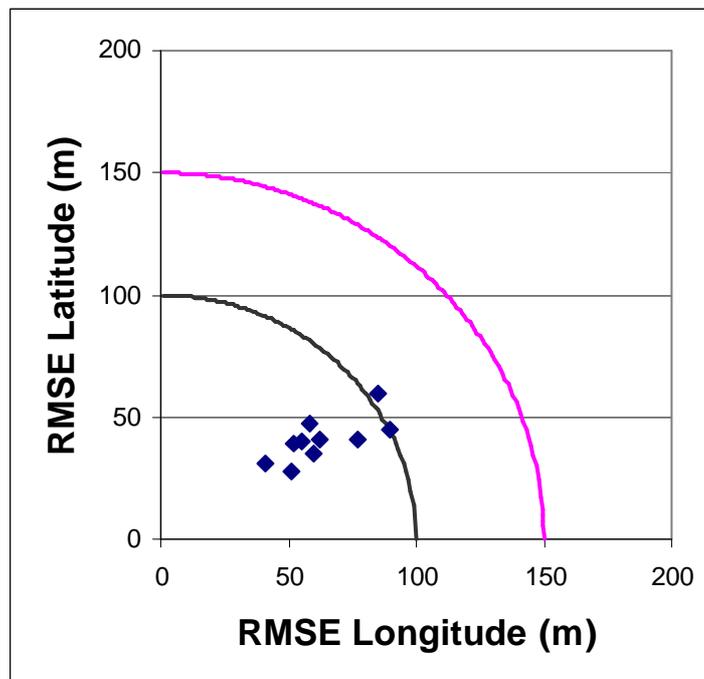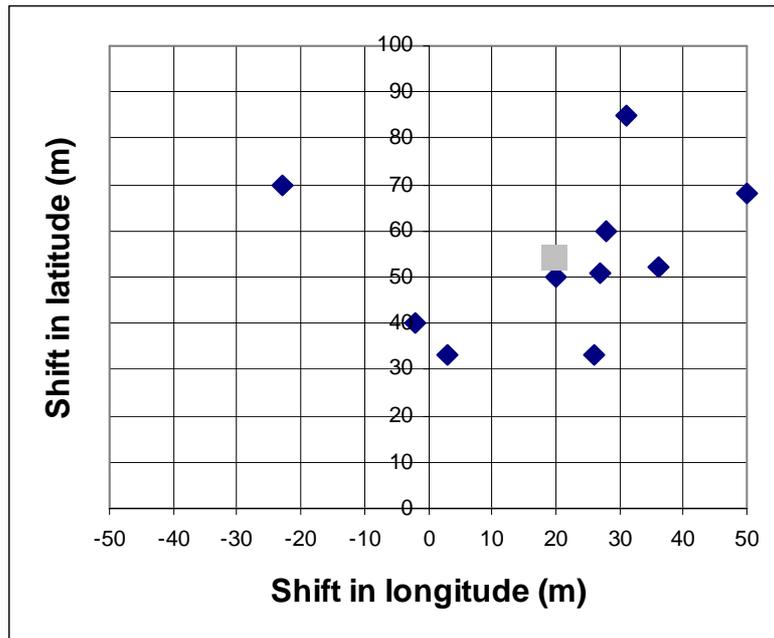| Site Name	Central site latitude	Topology	Number of data per season correctly geo-located and ortho-rectified			
			Winter	**Spring**	**Summer**	**Autumn**
Madagascar	20°S	Stressed relief	0	5 (10 pairs)	6 (15 pairs)	4 (6 pairs)
Tunisia	27°N	Desert	4 (6 pairs)	5 (10 pairs)	4 (6 pairs)	3 (3 pairs)
Spain-Morocco	35°N	Stressed relief	5 (10 pairs)	5 (10 pairs)	4 (6 pairs)	4 (6 pairs)
Romania-Ukraine	45°N	Flat land + some mountainous areas	0	6 (15 pairs)	6 (15 pairs)	4 (6 pairs)
North Europe (Poland-Sweden)	55°N	Flat land	0	4 (6 pairs)	5 (10 pairs)	4 (6 pairs)

Table 2 - Global relative accuracy results (unit: meter)

	Mean	Standard deviation	Minimum	Maximum
RMSE Latitude	33.6 m	21.1 m	13.4 m	130.5 m
RMSE Longitude	39.2 m	23.3 m	12.1 m	170.2 m
RMSE Total	51.6 m	26.3 m	26.3 m	214.4 m

Table 3 - Global absolute accuracy results with LANDSAT products (unit: meter)

	Mean	Standard deviation	Minimum	Maximum
Mean difference in latitude	19.1 m	22.2 m	-23.2 m	49.7 m
Mean difference in longitude	56.4 m	17.8 m	36.1 m	85.1 m
Standard deviation of differences in latitude	31.0 m	2.9 m	24.4 m	34.1 m
Standard deviation of differences in longitude	31.1 m	6.3 m	21.8 m	41.2 m
RMSE in latitude	41.2 m	9.0 m	29.2 m	59.1 m
RMSE in longitude	65.0 m	16.4 m	42.2 m	90.6 m
RMSE Total	77.1 m	17.8 m	52.5 m	104.2 m

8 Acknowledgement

9 References

[1] R. Defries, M. Hansen and J.R.G. Townshend, "Global discrimination of land cover types from metrics derived from AVHRR Pathfinder data", *Remote Sensing of Environment*, vol. 54, n° 3, pp. 209-222, Dec. 1995.

[2] M. Hansen, R. DeFries, J.R.G. Townshend, and R. Sohlberg, "Global land cover classification at 1km resolution using a decision tree classifier", *International Journal of Remote Sensing*, vol. 21, n° 6, pp. 1331-1365, Apr. 2000.

[3] M.A. Friedl, D.K. McIver, J.C.F. Hodges, X.Y. Zhang, D. Muchoney, A.H. Strahler, C.E. Woodcock, S. Gopal, A. Schneider, A. Cooper, A. Baccini, F. Gao, and C. Schaaf, "Global land cover mapping from MODIS: Algorithms and early results", *Remote Sensing of Environment*, vol. 83, n° 1-2, pp. 287-302, Nov. 2002.

[4] E. Bartholomé and A. Belward, "GLC2000: a new approach to global land cover mapping from Earth observation data", *International Journal of Remote Sensing*, vol. 26, n° 9, pp. 1959-1977, May 2005.

[5] S. Fritz, E. Bartholomé, A. Belward, A. Hartley, H.J. Stibig, H. Eva, "Harmonization, mosaicking, and production of the Global Land Cover 2000 database", Office for Official Publications of the European Communities, Luxembourg, EUR 20849, 2003.

[6] B. Holben, "Characteristics of maximum value composite images from temporal AVHRR data", *International Journal of Remote Sensing*, vol. 7, n° 11, pp. 1417-1434, Nov. 1986.

[7] M. Leroy and J.L. Roujean, "Sun and view angle corrections on reflectances derived from NOAA/AVHRR data", *IEEE Trans. Geo. Rem. Sen.*, vol. 32, n° 3, pp 684-697, May 1994.

[8] A.H. Strahler, L. Boschetti, G.M. Foody, M.A. Friedl, M.C. Hansen, M. Herold, P. Mayaux, J.T. Morisette and S.V. Stehman, "Global Land Cover Validation: Recommendations for Evaluation and Accuracy Assessment of Global Land Cover Maps", Office for Official Publications of the European Communities, Luxembourg, GOFC-GOLD Rep. 25, Mar. 2006.

[9] G.W. Rosborough, D. Baldwin and W.J. Emery, "Precise AVHRR image navigation", *IEEE Trans. Geo. Rem. Sen.*, vol. 32, n° 3, pp. 644-657, May 1994.

[10] J.F. Moreno and J. Melia, "A method for accurate geometric correction of NOAA AVHRR HRPT data", *IEEE Trans. Geo. Rem. Sen.*, vol. 31, n°1, pp. 204-226, Jan. 1993.

[11] D. Shin, J.K. Pollard and J. P. Muller "Accurate geometric correction of ATSR images", *IEEE Trans. Geo. Rem. Sen.*, vol. 35, n° 4, pp. 997-1006, Jul. 1997.

[12] C.T. Mutlow, A.M. Zavody and D.T. Llewellyn-Jones, "The Along Track Scanning Radiometer (ATSR) - Global Validation Results", in *Proc. of the 2nd ERS-1 Symposium, Space at the service of our environment,* Hamburg, Oct. 1993, pp. 1245-1249.

[13] S. Sylvander, P. Henry, C. Bastien-Thiry, F. Meunier, and D. Fuster, "VEGETATION Geometrical Image Quality", in G. Saint, V. P. S., ed., VEGETATION 2000 conference, 2 years of operation to prepare the future, Lake Maggiore - Italy, Apr. 2000.

[14] P.Y. Deschamps, F.M. Bréon, M. Leroy, A. Podaire, A. Bricaud, J.-C. Buriez, and G. Sèze, "The POLDER mission: instrument characteristics and scientific objectives", *IEEE Trans. Geo. Rem. Sen.*, vol. 32, n°3, pp. 598-615, May 1994.

[15] R. Wolfe, M. Nishishima, A. J. Fleig, J.A. Kuyper, D.P. Roy, J.C. Storey and F.S. Pratt, "Achieving sub pixel geolocation accuracy in support of MODIS land science", *Remote Sensing of Environment*, vol. 83, n°1-2, pp. 31-49, Nov. 2002.

[16] X. Xiong, N. Che, and W. Barnes, "Terra MODIS on-orbit spatial characterization and performance", *IEEE Trans. Geo. Rem. Sen.*, vol. 43, n° 2, pp. 355-365, Feb. 2005.

[17] V. Jovanovic, M.A. Bull, M.M. Smyth, and J. Zong, "MISR in flight camera geometric model calibration and geo-rectification performance", *IEEE Trans. Geo. Rem. Sen.*, vol. 40, n°7, pp. 1512-1519, Jul. 2002.

[18] V. Jovanovic, C. Moroney, and D. Nelson, "Multi-angle geometric processing for globally geo-located and co-registered MISR image data", *Remote Sensing of Environment*, vol. 107, n°1-2, pp. 22-32, Mar. 2007.

[19] W.E. Purdy, P.W. Gaiser, G.A. Poe, E.A. Uliana, T. Meissner, and F.J. Wentz, "Geolocation and pointing accuracy analysis for the WindSat Sensor", *IEEE Trans. Geo. Rem. Sen.*, vol. 44, n°3, pp. 496-505, Mar. 2006.

[20] G.A. Poe and R.W. Conway, "A study of the geolocation errors of the special sensor microwave/imager (SSM/I)", *IEEE Trans. Geo. Rem. Sen.*, vol. 28, n°5, pp. 791-799, Sep. 1990.

[21] D. Roy, "The impact of mis-registration upon composited wide field of view satellites and implications for change detection", *IEEE Trans. Geo. Rem. Sen.*, vol. 38, n°4, pp. 2017-2032, Jul. 2000.

[22] B. Tan , C.E. Woodstock, J. Hu, P. Zhang, M. Ozdogan, D. Huang, W. Yang, Y. Knyazikhin, and R. B. Myneni, "The impact of gridding artefacts on the local spatial properties of MODIS data: implications for validation, compositing, and band to band registration across resolutions", *Remote Sensing of Environment*, vol. 105, n°2, pp. 98-114, Nov. 2006.

[23] Y. Carmel, "Characterizing location and classification error patterns in time-series thematic maps", *IEEE Trans. Geo. Rem. Sen. Letters*, vol. 1, n°1, pp. 11-14, Jan. 2004.

[24] K.T. Weber, J. Théau, and K. Serr, "Effect of co-registration error on patchy target detection using high resolution imagery", *Remote Sensing of Environment*, vol. 112, n°3, pp. 845-850, Mar. 2008.

[25] J.R.G. Townshend, C.O. Justice, C. Gurney, and J. McManus, "The impact of mis-registration on change detection", *IEEE Trans. Geo. Rem. Sen.*, vol. 30, pp. 1054-1060, Sep. 1992.

[26] X. Dai and S. Khoram, "The effects of image mis-registration on the accuracy of remotely sensed change detection", *IEEE Trans. Geo. Rem. Sen.*, vol. 36, n° 5, pp. 1566-1577, Jul. 1998.

[27] P. Goryl and S. Saunier, "MERIS absolute geolocation status", ESA-GAEL, contract n°15993/02/I-LG, Tech. Rep. Issue 3, Apr. 2006.

[28] P. Goryl et al. "MERIS products quality status report: MEGS7.4 and IPF5", Tech Rep. Issue 1, Mar. 2006.

[29] L. Bourg and F. Etanchaud, "The AMORGOS MERIS CFI (Accurate MERIS Ortho Rectified Geolocation Operational Software)", *Software User Manual and Interface Control Document*, Tech. Rep. PO-ID-ACR-GS-003, Issue 3, Feb. 2007.

[30] M. Bouvet, "Intercomparison of ACE and SRTM 30 global digital elevation model at global and regional scale", ESA/ESTEC, Issue 2.0, Oct. 2004.

[31] L. Bourg and the ACRI MERIS Team, "MERIS Level 1 Detailed Processing Model, parameters data list", Tech. Rep. PO-TN-MEL-GS-002, Oct. 2006.

[32] T.G. Farr, et al., "The Shuttle Radar Topography Mission", *Rev. Geophys*, 45, RG2004, 2007, doi:10.1029/2005RG000183.

[33] P. A. M Berry, R. D. Hilton, C. P D. Johnson,.R.A. Pinnock, "ACE: A New Global Digital Elevation Model Incorporating Satellite Altimeter Derived Heights", European Space Agency, ERS-ENVISAT Symposium, Gothenburg, Sweden, Oct. 2000.

[34] G.Sotis, "EnviSat-1 Product Specifications, Volume 14: RA-2 Product Specifications", PO-RS-MDA-GS-2009, Issue 3, Revision P, Dec. 2006.

[35] F. G. Lemoine, S. C. Kenyon, J. K. Factor, R.G. Trimmer et al.,"The Development of the Joint NASA GSFC and NIMA Geopotential Model EGM96", NASA Goddard Space Flight Center, Greenbelt, Maryland, 20771 USA, Jul. 1998.

[36] S. Riazanoff, S. Mbaye, C. Demange, and S. Delwart, "ENVISAT MERIS Geometry Handbook", Tech. Rep. VT-P194-DOC-001-E, Issue 1.5, Jul. 2005.

[37] S. Baillarin, A. Bouillon, M. Bernard, and M. Chikhi, "Using a three dimensional spatial database to orthorectify automatically remote sensing images", in *ISPRS Workshop on Service and Application of Spatial Data Infracstructure*, , pp. 89-93, Hangzhou, Oct. 2006.

[38] S. Baillarin, J.P.Gleyzes, J.M. Delvit, A. Bouillon, E. Breton, and L. Cunin, "Validation of an automatic image orthorectification processing", in *Proceedings of IGARSS,* pp. 1398-1401, Anchorage, 2004,.

[39] J. Inglada and A. Giros, "On the possibility of automatic multisensor image registration", *IEEE Trans. Geo. Rem. Sen.*, vol. 42, n°10, pp. 2104-2120, Oct. 2004.

[40] J. Inglada, V. Muron, D. Pichard, and T. Feuvrier, "Analysis of artefacts in sub pixel remote sensing image registration", *IEEE Trans. Geo. Rem. Sen.*, vol. 45, n°1, pp. 254-264, Jan. 2007.

[41] K.V. Khlopenkov and A.P. Trishchenko, "Implementation and evaluation of concurrent gradient search method for reprojection of MODIS level 1B imagery", *IEEE Trans. Geo. Rem. Sen.*, vol.46, n°7,pp. 2016-2027, July 2008.

[42] M. Vanda Nunes de Lima, "IMAGE2000 and CLC2000: products and methods", EUR21757, ISBN 92-894-9862-5, EC-JRC, 2005.

[43] C.J. Tucker, D. Grant, and J.D. Dykstra, "NASA's Global Ortho-rectified Landsat Data Set", *Photogrammetric Engineering & Remote Sensing*, vol. 70, n° 3, pp. 313-322, 2004.

[44] P. Bicheron, M. Huc, C. Henry, S. Bontemps et al, "GlobCover : Products Description Manual", Issue 2, Rev. 2, Dec. 2008.

10 Authors Biographies

Patrice Bicheron received a Ph.D. in 1997 on the continental biosphere dynamic from University Paul Sabatier, Toulouse, France. He is currently working with Spot Image, a subsidiary of EADS/Astrium where a portion of his work is directed towards the development of agro-environmental applications. From 1998 to 1999, he was a Postdoctoral Fellow with the French Space Agency (CNES). His main research included the use of the POLDER instrument for vegetation monitoring. In 2000, he joined SCOT, a subsidiary of CNES, to develop applications using low resolution earth observations (VEGETATION, AVHRR). From 2002 until 2008, he participated to the French Land Surface Thematic Centre POSTEL where he was deputy manager of the EU/FP7-CYCLOPES project for the development of global biophysical products from multi-sensor observations. He was also manager of the ESA-GlobCover project providing the first global land cover map at 300-meter spatial resolution using ENVISAT/MERIS observations.

Virginie Amberg received her Ph.D. in 2005 in the signal processing field with a special interest to the use of SAR images. She is currently with the French Space Agency (CNES) in the field of optical image quality. From 2005 to 2007, she was working for Magellium, participating in several projects dealing with geometric images accuracy.

Ludovic Bourg received his Ph.D. degree in remote sensing from the University of Paris VII (France) in 1995. He joined ACRI-ST, a French R&D SME, in 1995 and has been working on optical remote sensing projects since then, with particular focus on the MERIS mission for the European Space Agency (ESA). He was in particular in charge of the definition of the Level 1 and Calibration algorithms, and the development of the associated software. Around 2000 he took the overall lead of the MERIS processing chain definition up to Level 2, including the co-ordination of several contributing laboratories. He was deeply involved in the commissioning of MERIS and is still presently in charge of managing the CAL/VAL activities and the evolutions of the MERIS algorithms. He has defined in particular the algorithms of the AMORGOS post-processing tool described in the present paper and supervised the tool development for ESA. These past three years, he has increased his involvement in the definition of next generation European optical sensors, like OLCI on-board Sentinel-3.

David Petit received his Ph.D. from University Paul Sabatier, Toulouse, France in the field of high resolution radar interferometry in 2004. His current position as Head of Research and Development at Magellium leads him to manage several projects in various fields of remote sensing application, 1D, 2D and 3D image processing or robotics methods.

Mireille Huc
Not Available

Carsten Brockmann holds a diploma in oceanography and a Ph.D. in Earth Science. He specialised in remote sensing and informatics early in his professional career. He was working at the University Hamburg, the GKSS Research Centre and the European Space Agency as remote sensing expert before he founded SCICON - Brockmann und Kleeberg GbR in 1994 and later Brockmann Consult in 1999. In 2001 he founded the Brockmann Consult GmbH which provides commercial software solutions for environmental processing systems. As managing director of the company he is responsible for all strategic decisions. He is actively involved in many projects for the company, notably all projects related with software for managing the data of the spaceborne sensor MERIS onboard the ESA satellite ENVISAT.

Bastien Miras
Not Available

Olivier Hagolle received his degree from the Ecole Supérieure d'Electricité, Gif-Sur-Yvette in 1990. Since 1990, he has been with the French Space Agency (CNES). From 1990 to 2002, he focused on satellite image quality and optical sensors calibration methods. In 2002-2004, he developed algorithms for the correction of directional effects for low resolution optical instruments such as VEGETATION, AVHRR, MERIS. Since 2004, he is with the Centre d'Etudes Spatiales de la Biosphère (CESBIO), Toulouse, France where he coordinates the level 2 specifications for the Venµs sensor, which combines high resolution, frequent revisit, and constant viewing angles. He focuses on the development of methods for estimating the aerosol optical depth over terrestrial surfaces.

Franck Ranera received in 1999 a Specialized Masters in Remote Sensing from the University Paul Sabatier, Toulouse, France. He is currently with Spot Image, a subsidiary of EADS/Astrium where a portion of his work is directed towards the management of projects related to risk fields. From 1999 to 2008, he was with Serco in Italy where he supported many ESA projects related to risk and Application fields (Globcarbon, GLOBCOVER, Medspiration, Urbex, CoastChart). His main task was to ensure the correct implementation of the project with respect to the technical requirements. He was responsible of the project technical side, reporting directly to the ESA project officer. He conducted several acceptance test of the projects production's chain and liaised frequently with scientific groups to ensure product reliability and consistency.

Marc Leroy obtained a Ph.D. from Paris VII University in 1980 in the field of radiatively driven stellar winds. He became Research Associate of Observatoire de Paris in 1981 and worked in the field of theoretical plasma physics of the Earth's bow shock, both at Observatoire de Paris and at the University of Maryland. He joined the French Space Agency (Centre National d'Etudes Spatiales) in Toulouse in 1985 and has worked since then as a CNES Engineer. He worked first on calibration activities associated to the SPOT program, and became in 1990 the Head of the Department of Image Quality in the CNES Image Processing Division. He joined CESBIO (Toulouse) in 1993 with a specific interest in the physics of remote sensing measurements in the optical domain, and in charge there of the development of algorithms of land surface products of the POLDER/ADEOS instrument. He joined MEDIAS-France in 2001 as Head of the Land Surface

Thematic Centre POSTEL. From 2001 to 2008, he developed POSTEL and its Service Centre and took a significant role in several important European projects, in particular GEOLAND and GLOBCOVER.

Olivier Arino completed his academic education in 1990 with a Ph.D. degree in Physics with speciality in Remote Sensing from the Institut National Polytechnique de Toulouse, France. After two years as a postdoctoral fellow with the International Geosphere Biosphere Program and the European Commission, he joined the European Space Agency in 1991. His current position as Head of the Projects Section in the Science Applications and Future Technologies Department of the Earth Observation Programme Directorate leads him to manage the Data User Programme in close collaboration with user communities (e.g. 300+ user organisations involved) and the relevant institutional communities, such as the United Nations Food and Agricultural Organisation, the United Nation Environment Programme and the European Environment Agency. He initiated the GlobSeries that are considered as precursors to the climate change initiative called "Global Monitoring of the Essential Climate Variable" recently funded by the Agency's ministers. He also worked closely with the International Environmental Conventions secretaries and users on climate change, desertification, biodiversity, wetlands and world heritage. He has authored or co-authored 110 scientific publications in the field of albedo, fire, vegetation, agriculture, land cover, sea surface temperature, and was nominated for the best European paper in open literature in 1992. He has acted as a reviewer for the International Journal of Remote Sensing, IEEE Transactions on Geoscience and Remote Sensing, Remote Sensing of the Environment and others. He is a member of international science groups in sea surface temperature, forest and land cover. Olivier Arino was appointed Senior Advisor in ESA in 2008.

Steve Delwart

Not Available.